A 420 GHz 2D Beam-steering TX in 40 nm CMOS Technology

Dragan Simic[1,2], Patrick Reynaert[2]
[1]Semiwave, Belgrade, Serbia [2]KU Leuven ESAT/MICAS, Leuven, Belgium
dragan.simic@semi-wave.com, patrick.reynaert@kuleuven.be

***Abstract*— This paper presents a 420 GHz 2D beam-steering transmitter designed for THz imaging applications and fabricated in 40 nm CMOS technology. Radiating on the chip back side through a high-resistivity hyper-hemispherical Silicon lens, this TX consists of 24 antenna elements. It is based on a multiplier-chain architecture and relies on both antenna-lens center displacement and phase-shifting beam-steering principles. It achieves the measured beam steering ranges of 40° and 50° in E and H planes, respectively, measured peak EIRP of 9.8 dBm with 3dB BW of 28 GHz and the measured 10 MHz phase noise of -120.2 dBc/Hz.**

***Index Terms*— THz TX, THz imaging, 2D beam steering, phase shifting, multiplier chain, CMOS**

I. Introduction

The last two decades have been a breakthrough period in the implementation of Silicon-based circuits operating in the THz frequency range (300 GHz-3 THz). Application-wise, THz imaging has emerged as the most promising domain for the use of such chips, with several research system demonstrations (both amplitude and phase based) and a few industrial players actively working in this field. Offering intrinsically high resolution, these systems find applications in numerous domains, from security screenings and medical and biological non-invasive scanning to industrial positioning systems.

Depending on the receiver architecture, two fundamental working approaches can be identified in THz imaging systems (Fig. 1): (a) single-pixel RX, with a focused beam TX and mechanical scanning of the object, and (b) pixel array RX, with a wide beam TX that captures the object image in a single shot. The first principle offers a high SNR at the RX pixel input, low design complexity and high imaging resolution (limited by diffraction). However, it requires a long imaging time due to mechanical scanning. The second approach gives much faster imaging time. However, it operates at lower SNR at the detector inputs, leading to larger system complexity and RX baseband requirements. To address the weaknesses of these two principles, a third technique (Fig. 1) is proposed that relies on a high-directivity beam-steering TX. It maintains a high SNR at the RX input while performing electrical scanning of the object, significantly reducing overall imaging time. This paper presents such a transmitter, developed for high-resolution fast imaging systems.

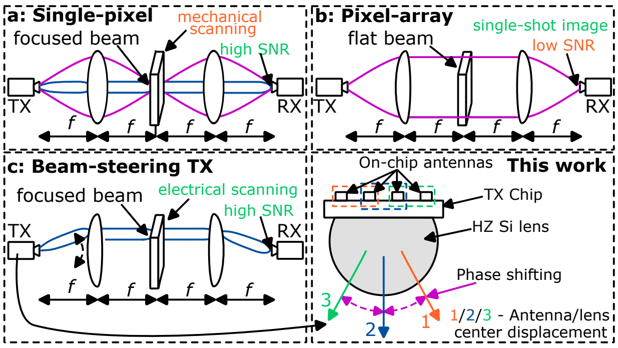

Fig. 1: Conventional and proposed imaging principles with the used beam-steering techniques.

The designed TX is implemented as an octagonal array of 24 radiating elements, with four elements (2 x 2 subarray) active simultaneously. This array pattern is chosen to illuminate the complete collimating lens required for electrical scanning (Fig. 1). Each radiating path is based on a tripler-last topology. The choice of multiplier as the THz-generating element, rather than a free-running or injection-locked oscillator, is made to achieve good phase noise and BW performance. This is done because the presented transmitter is implemented for use in a phase imaging system, together with the receiver from [1]. The high directivity radiation is achieved by the use of a high-resistivity hyper-hemispherical Silicon lens attached to the chip back side. This technique is used to avoid BW reduction and the need for very large antenna arrays necessary to achieve similar directivities with front-side radiators. Beam steering is achieved through two methods: antenna-lens center displacement and phase shifting between adjacent antenna elements (Fig. 1). The first one is based on using only 2 x 2 subarrays during the operation. The displacement between the center of such a subarray and the lens center results in larger, fixed beam-steering steps. The finer steering angles are achieved by introducing phase shifts between the 2 x 2 elements. Using the mentioned techniques, the measured beam steering ranges of 40° and 50° are achieved in E and H planes, with the measured peak EIRP of $9.8\,\mathrm{dBm}$ and $10\,\mathrm{MHz}$ phase noise of $-120.2\,\mathrm{dBc/Hz}$.

979-8-3195-0631-3/26/$31.00 ©2026 IEEE

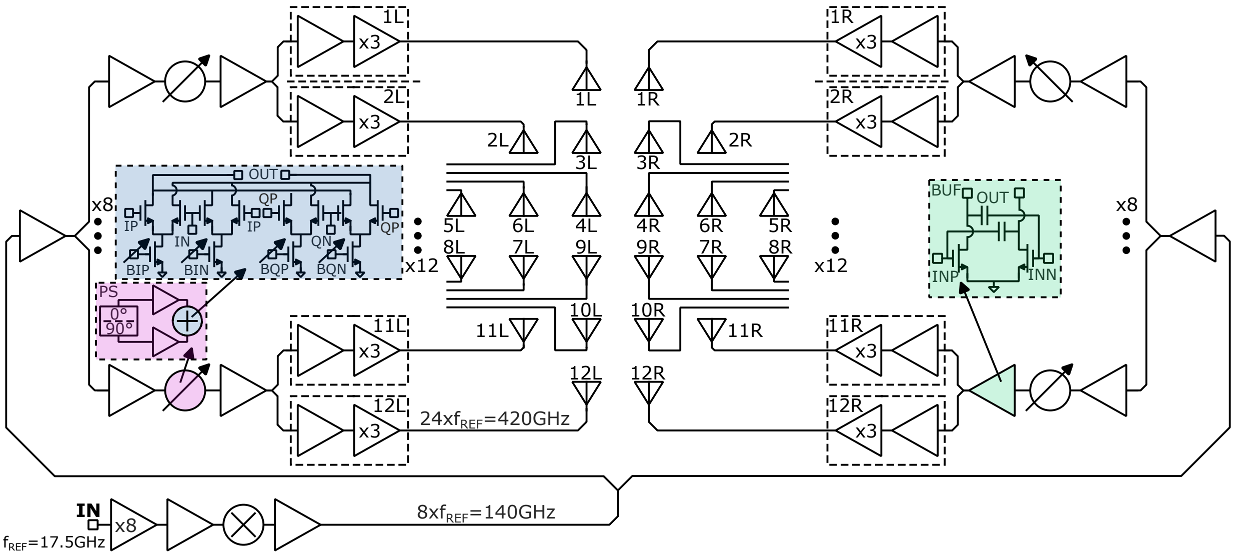

Fig. 2: The complete block-level schematic of the designed $420\,\text{GHz}$ beamformer.

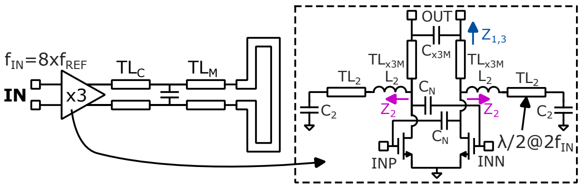

Fig. 3: The schematic of a single radiating path.

II. TX Beamformer Design

Figure 2 presents a complete TX architecture (for simplicity, all connections are drawn single-ended, whereas they are differential in the implemented chip). It consists of 24 radiating paths, all based on a tripler-last topology. The input signals for these triplers are generated starting from a $17.5\,\text{GHz}$ off-chip reference (f_{OUT}/f_{REF}=24). This reference is multiplied by 8 and provided to the buffer-splitter network to deliver $140\,\text{GHz}$ signals to 16 phase shifters (buffers and phase shifters shown in Fig. 2). Phase shifters outputs are further split into two to create a total of 32 $140\,\text{GHz}$ output paths. Eight of these are terminated, while the other 24 are further amplified and brought to THz triplers. The reason for such a network is to guarantee symmetry among all the radiating paths (splitting is always done one to two). In addition, a $140\,\text{GHz}$ mixer is inserted into the chain to enable low-frequency TX modulation (to avoid the influence of RX flicker noise on the overall imaging system performance [1]).

A main difficulty when implementing a multiplier-based on-chip THz 2D beam-steering array is that the spacing between antennas is too small to accommodate the multipliers and their feeding structures (λ/2 at $420\,\text{GHz}$ in Silicon is $104\,\mu\text{m}$). This limits the array's scalability and often dictates only a 1D array implementation. In this work, THz triplers are implemented outside of the antenna array area, with each antenna fed by the $50\,\Omega$ differential transmission lines. Figure 3 shows individual radiating paths schematics, with TL_C denoting the connecting transmission lines. The antennas are designed as folded dipoles and spaced for $127.4\,\mu\text{m}$ in E plane and $133.5\,\mu\text{m}$ in H plane. Since for imaging uses the needed steering angles are around $\pm 30°$, or often less (dictated by the collimating lenses' focal distance to diameter ratio, Fig.1), this spacing could be larger than λ/2, increasing the total steering range. Including the antenna matching network, the total simulated antenna efficiency ranges from $20\,\%$ to $25\,\%$, depending on the lens size. There are a total of six different transmission lines in the designed TX (the antenna array is centrally symmetric), where the lengths of five of these lines are equalized to $510\,\mu\text{m}$, with the simulated loss of $1.9\,\text{dB}$. The length of the sixth line is equal to $140\,\mu\text{m}$ with the simulated loss of $0.6\,\text{dB}$. The difference in these losses can be tuned by individual tuning of the tripler output powers, while the phase difference can be tuned using phase shifters.

A detailed schematic of a single radiating path, including the THz tripler schematic, is shown in Fig. 3. It is based on the pseudo-differential capacitively neutralized differential pair, with the load impedances of the fundamental, second, and third harmonics optimized to maximize third harmonic output power ([1]). The fundamental and third harmonic outputs are differential, with the load impedances optimized through a matching network

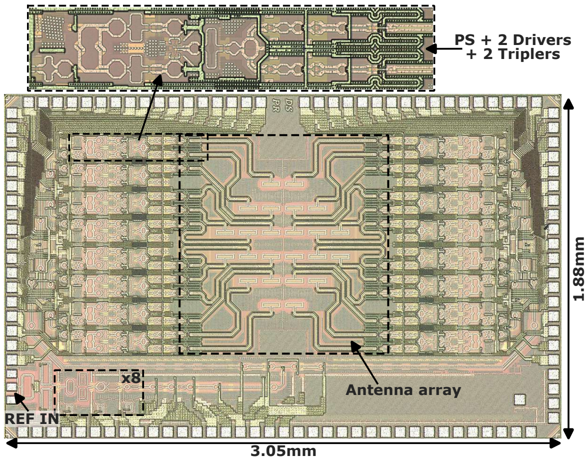

Fig. 4: Chip photo of the designed 420 GHz transmitter.

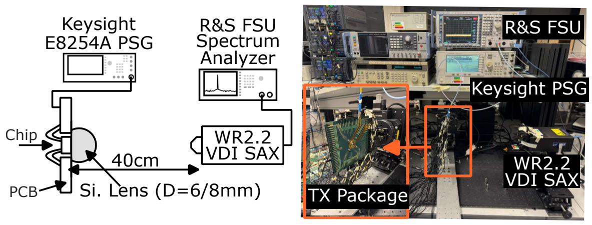

Fig. 5: The block scheme and photo of the used measurements setup.

between the tripler and the $50\,\Omega$ antenna transmission line. The common-mode second harmonic load impedance is provided through AC-shorted $\lambda/2$ (at $280\,\mathrm{GHz}$) transmission line (TL_2) in series with an inductance (L_2). To fit these transmission lines into the limited area, they are meandered and laid out in parallel to the signal flow. The width of a single radiating path (including driving amplifier and the THz tripler) is $75\,\mu\mathrm{m}$. The simulated tripler third harmonic output power is $-9\,\mathrm{dBm}$. Together with the transmission line loss and antenna efficiency, and taking into account four elements working simultaneously (perfect combining assumed), this results in a total simulated TX radiated power between $-11.9\,\mathrm{dBm}$ and $-10.9\,\mathrm{dBm}$ (depending on the lens size).

III. Measurement Results

The presented transmitter is fabricated in standard $40\,\mathrm{nm}$ bulk CMOS technology with dimensions of $3.05\,\mathrm{mm}$ x $1.88\,\mathrm{mm}$ (Fig. 4). A high-resistivity hyper-hemispherical Silicon lens (without an anti-reflective coating) is glued to its back side, with the DC signals and the $17.5\,\mathrm{GHz}$ reference connected via bond wires. The size of the lens depends on the application, with larger lenses providing greater directivity and smaller ones offering a

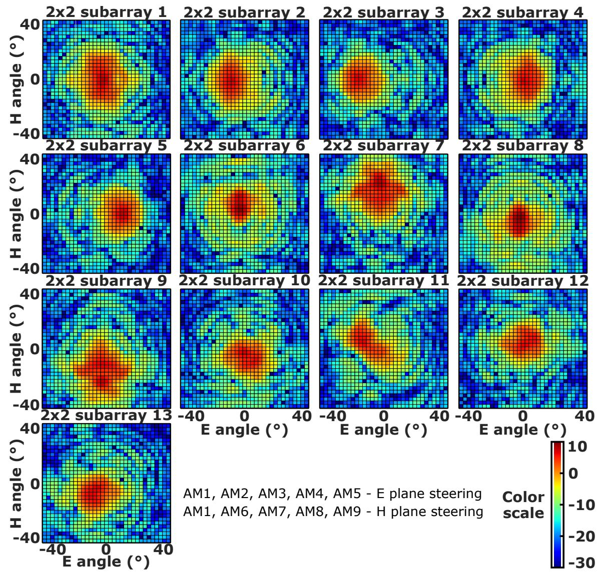

Fig. 6: The measured 2D radiation patterns for $8\,\mathrm{mm}$ lens diameter and different 2 x 2 subarrays (no phase shifting).

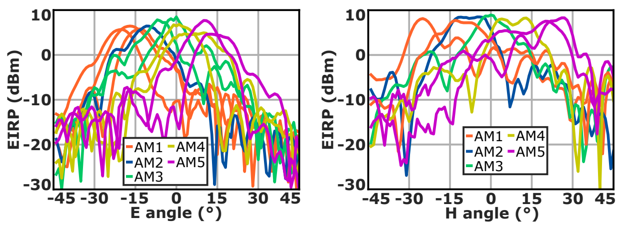

(a) (b)

Fig. 7: The measured 1D radiation patterns for $8\,\mathrm{mm}$ lens diameter in E and H planes (with phase shifting). Different colors indicate which 2 x 2 subarray is active.

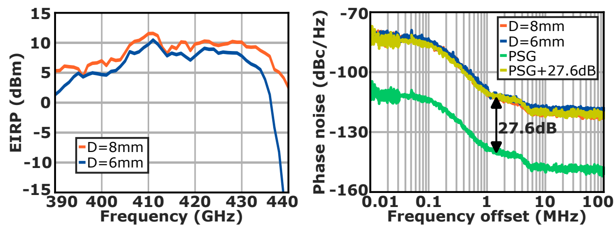

(a) (b)

Fig. 8: (a) The measured TX maximum EIRP versus RF frequency for the lens diameter of $8\,\mathrm{mm}$. (b) The measured TX phase noise for the lens diameter of $8\,\mathrm{mm}$.

larger steering range ([7]). The designed TX is evaluated using two lens sizes, $8\,\mathrm{mm}$ diameter with a thickness of $4.6\,\mathrm{mm}$ and $6\,\mathrm{mm}$ diameter with a thickness of $3.4\,\mathrm{mm}$.

TABLE I: Comparison of Silicon based state-of-the-art beam-steering THz transmitters

	This work	**[2]**	**[3]**	**[4]**	**[5]**	**[6]**
Technology	**40 nm CMOS**	65 nm CMOS	65 nm CMOS	40 nm CMOS	45 nm SOI	65 nm CMOS
Array size	**24 elements**	4x4	25 elements	4x1	8x1	4x4
Topology	**Mult. chain**	Coupl. Osc.	Ink. Locked Osc.	Inj. Locked Osc.	Mult. chain	Coupl. Osc.
Frequency (GHz)	**420**	416	310	531.5	390	338
BW (GHz)	**28**	7.1*	36	4.8*	33	7.1*
Steering range	**50/40**	60/60	36/0	60/0	75/0	45/50
EIRP (dBm)	**9.8**	14	20.3	2.3	8	17.1
P_{RAD}(dBm)	**-13.9**	-3	6.5	-12	/	-0.9
PDC (mW)	**930**	1450	2100	260	1500	1540
Phase noise (1 MHz)	**-110.5**	-88	/	-99+	/	-93
Phase noise (10 MHz)	**-120.2**	-100+	/	-105+	/	/

*oscillator tuning range (not 3 dB BW) +graphically estimated

The photo and block diagram of the measurement setup are shown in Fig. 5. The designed TX is mounted on a two-axis rotational stage for full 2D measurements. Its input power is captured using the VDI WR2.2 RX module and the R&S FSU (previously calibrated by the VDI WR2.2 TX module and the Erickson PM5 power meter). The supply TX voltage is 1 V, and the measured power consumption (during operation) is 930 mW.

The measured 2D radiation patterns for 8 mm lens diameter and all the 2 x 2 subarrays are shown in Fig. 6 (phase shifters calibrated to radiate to the center of the active subarray). Figure 7 presents the measured 1D radiation patterns for 8 mm lens diameter in E and H plane. In this case, the large steering steps are achieved using the antenna-lens displacement technique, with intermediate steps obtained by phase shifting. For the 8 mm lens size the measured maximum EIRP is 11.6 dBm (at 411 GHz) and the measured EIRP at 420 GHz is 9.8 dBm. The measured beam-steering ranges are 40° and 50° in E and H planes. The measured directivity in the maximum EIRP case (based on 3 dB beamwidth formula) is 23.7 dBi, resulting in the measured radiated power of -13.9 dBm.

Figure 8(a) shows the measured EIRP versus frequency, showing the measured EIRP 3 dB BW of 28 GHz in the case of 8 mm diameter lens. Finally, the measured phase noise of the designed TX is shown in Fig. 8(b), with the measured phase noise of -110.5 dBc/Hz at 1 MHz and -120.2 dBc/Hz at 10 MHz. Together with the phase noise of the designed TX, Fig. 8(b) shows the measured phase noise of the 17.5 GHz input reference, illustrating the difference between the measured TX input and output phase noise being very close to the theoretical 27.6 dB (20log(24)), meaning that the designed TX has a very limited impact on the total phase noise performance.

IV. Conclusion

The measured performance of the presented TX is compared with state-of-the-art THz beam-steering arrays in Table I. The proposed design achieves the best phase noise performance, enabled by its multiplier-based architecture, and offers the second-largest bandwidth. Employing two beam-steering techniques, it provides a 2D steering range sufficient for imaging applications. To the best of the authors' knowledge, this work represents the first 2D multiplier-based THz beam-steering array. Combined with its precise 2D beam-steering capabilities, these results make the proposed TX well-suited for THz imaging applications based on electrical scanning.

References

[1] D. Simic, K. Guo, and P. Reynaert, "A 420-ghz sub-5-μm range resolution tx–rx phase imaging system in 40-nm cmos technology," *IEEE Journal of Solid-State Circuits*, vol. 56, no. 12, pp. 3827–3839, 2021.

[2] H. Saeidi, S. Venkatesh, C. R. Chappidi, T. Sharma, C. Zhu, and K. Sengupta, "A 4 × 4 steerable 14-dbm eirp array on cmos at 0.41 thz with a 2-d distributed oscillator network," *IEEE Journal of Solid-State Circuits*, vol. 57, no. 10, pp. 3125–3138, 2022.

[3] M. Yang and L. Wu, "A 298–334-ghz scalable injection-locked phased-array radiator with second-subharmonic-termination-assisted waveform formulation for power enhancement," *IEEE Journal of Solid-State Circuits*, pp. 1–12, 2025.

[4] K. Guo, Y. Zhang, and P. Reynaert, "A 0.53-thz subharmonic injection-locked phased array with 63- μ w radiated power in 40-nm cmos," *IEEE Journal of Solid-State Circuits*, vol. 54, no. 2, pp. 380–391, 2019.

[5] Y. Yang, O. D. Gurbuz, and G. M. Rebeiz, "An eight-element 370–410-ghz phased-array transmitter in 45-nm cmos soi with peak eirp of 8–8.5 dbm," *IEEE Transactions on Microwave Theory and Techniques*, vol. 64, no. 12, pp. 4241–4249, 2016.

[6] Y. Tousi and E. Afshari, "A high-power and scalable 2-d phased array for terahertz cmos integrated systems," *IEEE Journal of Solid-State Circuits*, vol. 50, no. 2, pp. 597–609, 2015.

[7] H. Jalili and O. Momeni, "A 0.46-thz 25-element scalable and wideband radiator array with optimized lens integration in 65-nm cmos," *IEEE Journal of Solid-State Circuits*, vol. 55, no. 9, pp. 2387–2400, 2020.